Scaling up the Throughput of Synthesis and Extraction in Droplet Microfluidic Reactors

Piotr M. Korczyk[1]*, Monika E. Dolega[2,3], Slawomir Jakiela[4], Pawel Jankowski[4], Sylwia Makulska[4] and Piotr Garstecki[4]*

[1]*Institute of Fundamental Technological Research, Polish Academy of Sciences, Pawinskiego 5B, 02-106, Warsaw, Poland*
[2]*University of Grenoble Alpes, LIPHY, F-38000, Grenoble, France*
[3]*CNRS, LIPHY, F-38000, Grenoble, France*
[4]*Institute of Physical Chemistry, Polish Academy of Sciences, Kasprzaka 44/52, 01-224, Warsaw, Poland*

Conducting reactions in droplets in microfluidic chips offers several highly attractive characteristics, among others, increased yield and selectivity of chemical syntheses. The use of droplet microfluidic systems in synthetic chemistry is, however, hampered by the intrinsically small throughput of micrometric channels. Here, we verify experimentally the potential to increase throughput via an increase of the scale of the channels. We use the results of these experiments characterizing the processes of (1) generation of droplets, (2) mixing in droplets, (3) inter-phase extraction, and (4) the yield of synthesis of pyrrole, to postulate a number of guidelines for scaling up the throughput of microfluidic droplet systems. In particular, we suggest the rules for maximizing the throughput via an increase of the size of the channels and via parallelization to optimize the throughput of synthesis against the cost of fabrication of the chips and against the kinetic requirements of specific reactions.

Keywords: flow chemistry, microfluidics, synthesis, emulsions, droplets

1. Introduction

In this paper, we analyze the strategies for increasing throughput of reactions conducted in droplets in microfluidic systems. In particular, we verify experimentally the rate and the stability of processes that are critical to the use of droplets as reaction beakers. We test these processes against the width of the channels, for widths ranging from 200 μm to 2 mm. We analyze the scaling laws of (1) formation of droplets, (2) mixing in droplets, (3) interphase transfer, and (4) yield of a chemical synthesis. We use the results of these screens to propose a number of design rules for microfluidic systems to maximize throughput for given kinetic requirements of reactions. These rules can guide optimization of throughput of droplet microfluidic systems for syntheses at laboratory and industrial scale.

1.1. History of Flow Reactors. The concept of continuous-flow reactors dates back to 1950s when the technique of segmented flow analysis (SFA) was developed in response to the demand for throughput in clinical diagnostics. System developed by Skeggs in 1957 [1] and later marketed by Technicon Co. aspired samples into tubing of millimetric diameter and segmented them by air bubbles to decrease dispersion of time of reaction and cross-contamination. As bubbles interfere with detection schemes, SFA was replaced in 1970s by flow injection analysis (FIA) [2] that uses single-phase flow. Integrated FIA microsystems [3] usually have planar format of systems of channels (of width of≈1 mm) and resemble the concurrent microfluidic chips.

The rapid development of microfluidic technologies prompted the visions of radical miniaturization of analytical techniques. In the 1990s, the existing technologies of chemical analysis – chromatography and electrophoresis – which already used capillaries of small cross-sections were translated into the format of integrated devices (chips) [4, 5]. Among other advantages, integration brings in the potential to execute complicated protocols [6].

1.2. Advantages of Microflow Reactors. In the beginning of 2000s, Thorsen [7] and Anna [8] demonstrated that confinement of streams of immiscible liquids and low Reynolds numbers can yield superb control over formation of monodisperse microdroplets. It has been quickly recognized [9] that microdroplets can serve as individual microreactors. The ability to conduct reactions within droplets has been intensively exploited in the recent years due to the following attractive characteristics [10–13]: (1) excellent reproducibility of formation of droplets, (2) fast (millisecond) mixing, (3) lack of dispersion of time of residence, (4) ease of control of the kinetics of reactions via the simple correspondence between the time of residence and the position in the channel, and (5) increased ratio of surface area to volume providing for efficient heat transfer (crucial for control of the highly exothermic or endothermic reactions) [14, 15] and for efficient mass transfer that is crucial for extraction or purification processes [16].

Of all techniques of flow-through reactors, droplet microfluidics offers probably the best combination of control and stability of processes and ease of interfacing various detection schemes [17–19]. As droplet microfluidic systems typically operate on droplets of volumes ranging from single pL (tens of micrometers in diameter) to single nL (small hundreds of micrometers), the technique is perfectly suited for analytical and screening applications where low consumption of liquids is beneficial. Still, the same advantages are highly desirable in syntheses, especially where yield and purity of product depend strongly on kinetic conditions [20], in reactions that are dangerous (e.g., include explosive substrates, intermediates or products) [21], or ones that use particularly expensive reagents or intermediates [22]. Single-phase systems have been widely reported (see for example review by Brivio et al. [23]) to yield increased rates of reaction, yields, and selectivities in comparison to traditional batch-syntheses. For example, Haswell et al. demonstrated that the aldol reaction between aldehydes and silyl enol ethers in the presence of tetrabutyl ammonium fluoride (TBAF) reaches completion in only 20 min while the batch reaction requires 24 h for the same result [24]. Haswell's group reported increased selectivity of the *cis* (Z) to *trans* (E) isomeric

* Authors for correspondence: piotr.korczyk@ippt.pan.pl, garst@ichf.edu.pl

ratio of the product of Wittig reaction [25]. The unique heat transfer properties of microreactors allow to safely conduct syntheses otherwise considered dangerous for exothermic properties and explosive character. A number of groups have carried out nitration reactions in microreactors, controlling both the yield and selectivity [26–28]. Loebbecke et al. developed a fully automated microfluidic plant for the synthesis of nitrate esters such as ethylene glycol dinitrate (EGDN), triethylene glycol dinitrate (TRENO), methyl nitrate (MN), trinitroglycerin (NGL), and other highly explosive compounds [29]. The yield, selectivity, and quality of products of many reactions depend on homogeneity [30] of solutions at the molecular level and thus on the efficiency of micromixing [31, 32]: as, e.g., Michaelis–Menten reactions [33], crystallization [34], or parallel reactions [35, 36].

1.3. Challenges in Scaling up the Throughput of Droplet Microreactors. As droplet microfluidics offers a range of advantages over single-phase microfluidics (i.e., faster mixing, faster interphase transfer, smaller dispersion in time of residence, etc.), the droplet systems may be particularly attractive for laboratory and industrial implementations of a range of syntheses. The application of droplet microfluidics to syntheses is, however, strongly hampered by the small throughput of these systems.

There are two general strategies to increase throughput of droplet systems: one is to increase the number of droplets created [37, 38] and processed in parallel. In this approach, numerous microfluidic modules are equally supplied with liquids. The parallelization and homogeneous distribution of liquids between all modules may be ensured by splitting the input flows between hierarchical structures of manifold channels [38] or by a circular arrangement of all base modules on the microfluidic chip [37]. The second is to increase the volume of each droplet. The idea to use larger droplets has been promoted by Engl et al. [39, 40] and Panizza et al. [41] for fabrication of millimetric solid objects using techniques similar to those proposed earlier for micrometric particles [42]. The same group demonstrated also the usefulness of droplet millifluidic systems for kinetic analyses of slow reactions [43]. Steinbacher et al. [44] presented simple mesofluidic droplet devices made of tubing, adapters, and needles that may be alternative to more expensive microfluidic systems.

The idea to use large channels is attractive because fabrication of millimetric channels is less expensive than microfabrication and because the maximum rate of flow can be expected to scale with the square of the width of the channel (because the speed of flow – and the capillary number, Ca – scales as $u = Q/w^2$; thus, keeping the speed (Ca) constant corresponds to $Q \propto w^2$). We will show below that this simple expectation is not true.

Further, because the aforementioned advantages of droplet systems rely strongly on features that are scale-dependant, i.e., relative importance of interfacial forces and effectiveness of convection and diffusion across the size of the droplet, the droplets cannot be enlarged to an arbitrarily large scale. It is thus important to characterize in detail how the crucial processes scale with the size of the channels and what the limits in the size of the droplets for maintaining the attractive process characteristics associated with the flow at the microscale are.

1.4. Outline of the Report. As there certainly are limits to the feasible size of the droplets, it is also obvious that obtaining large throughput may require both increasing the size of the droplets and constructing parallel systems for simultaneous processing. Thus, for every process, characterized by required throughput and desirable rates of mixing, chemical synthesis, or interphase transfer, there should be an optimum compromise between the extent of parallelization and choice of an appropriate scale of the individual channels.

The syntheses conducted in droplets in microfluidic channels involve a number of processes including formation of droplets, mixing of the content of droplets, extraction through the liquid–liquid interface, and the chemical reaction itself. As each of these processes is governed by different mechanisms and in principle may scale in a different manner with the size of the channels, we first characterize the throughput of each of these processes individually. The sections devoted to this analysis conclude with the scaling relations for each of the processes as a function of the size of the channels and the rate of flow of the liquids. Having the contributions from the individual components of the process, we then discuss the optimization of the design of droplet systems for chemical synthesis. We provide guidelines for maximization of throughput of syntheses in the context of geometrical similarity of microfluidic systems across length-scales, the cost of fabrication, throughput of a single junction, and requirements set by the kinetics of the reactions. We finally conclude the findings and list the experimental details.

Results and Discussion

2.1. Formation of Droplets. At low values of the capillary number (Ca = $\mu u/\sigma$, where μ and u are the viscosity and the superficial speed of the continuous phase and σ is the interfacial tension between the two liquids), both the T-junction [7] and the flow-focusing [8] generators form droplets in the squeezing regime [45–47]. Within this mode of formation of droplets, their volume (V) is a function only of the rates of flow of the two immiscible phases: $V \propto Q_d/Q_c$. At higher values of Ca, the shearing effects modify the scaling relation and introduce a power law dependence [48, 49] $V \propto Ca^{-\alpha}$, with α ranging between 0.1 and 0.3. Although a number of studies [46–56] examined the scaling of V with various parameters (geometry of the junction, speed of flow of fluids, viscosities and interfacial tension), none considered the dependence on the sheer scale (width) of the channels. Here, we used geometrically similar T-junction systems and flow-focusing junctions that had all channels of the same square cross-section and different widths w of the channels w=0.39, 0.61, 0.79, and 1.2 mm (Supporting Information [SI], Figure S1). We used hexadecane with 2% (w/w) Span80 as a continuous phase and distilled water as a droplet phase. In all experiments, we kept the ratio of the rate of flow of the droplet phase (Q_d) to the rate of flow of the continuous phase (Q_c) constant Q_d/Q_c=1.2.

Figure 1 shows the length L_d of droplets generated in the T-junction systems normalized by the width of the channel w as a function of Ca = $Q_c\mu/\sigma w^2$ (note that for elongated droplets confined by channel walls, the relation between length L and volume V is approximately linear). We observed that for Ca < $8°10^{-3}$, the data sets obtained for channels of different widths fall onto the same master relation. For higher values of the capillary number, the measurements do not overlap. We found that it impossible to find a single scaling for this data, i.e., the data does not fall onto a master curve when plotted as a function of, e.g., Reynolds or Weber numbers.

We also tested formation of droplets in systems comprising channels of widths of up to 4 mm. In the case of w=4 mm, we observed that droplet phase was flattened by gravity and we did not observe reproducible generation of droplets at all. We expect that for $w \leq 1.2$ mm, the droplets fill almost the whole cross-section of the channel, as the capillary length ($\lambda = (\sigma\ (\Delta\rho\ g)^{-1})^{0.5}$, where σ is the interfacial tension between the two liquids, $\Delta\rho$ is a density contrast and g is the gravitational acceleration) for the applied liquids is about 1.2 mm. In larger channels, gravity flattens the droplets and
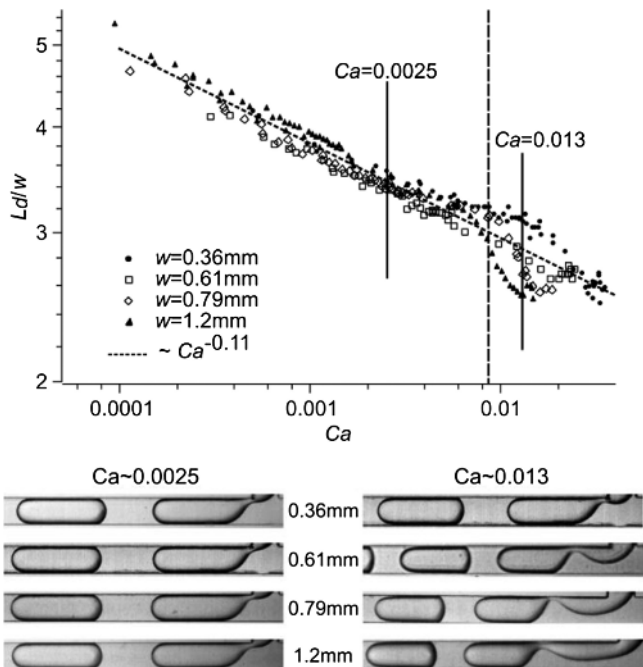
Figure 1. (top) Nondimensional length (L_d/w) of droplets (slugs) formed in T-junctions of different width (w) as a function of the value of the capillary number. (bottom) Micrographs illustrating that, at low values of Ca, the T-junctions of different size operate in a similar manner, while, at large values, the scaling with Ca does not fully determine the operation of the system (all micrographs were taken just before detachment of a droplet)

Figure 2. (top) Micrographs of the dripping and jetting regime in the T-junctions of different sizes. (bottom) The normalized length of the tip of droplet phase ($L_t - L_d)/w$ as a function of Q_c, where L_t is the length of the droplet phase stream and L_d is the length of a droplet. Width of the channel w: circles — 0.39 mm, squares — 0.61 mm, triangles — 0.79 mm, and diamonds — 1.2 mm. For each value of w, we estimated the rate of flow Q_{jet} at which $(L_t - L_d)/w = 3$. The inset shows the scaling of Q_{jet} with w for the T-junction (open symbols) and for the flow-focusing device (solid symbols)

causes vertical separation of both liquids into parallel layers, resulting in the loss of strictly plug-like character of the flow. This facilitates the flow of the continuous liquid past a growing droplet and modifies the condition for breakup [53, 57]. Thus, as could be expected, gravitational effects impose an upper limit (of $w = 1.2$ mm) on the size of the channels for formation of droplets for the liquids used in these particular investigations. Note that this is not a general rule as the capillary length depends on the character of the liquids. In the further sections concerning mixing, extraction, and the synthesis within droplets, we used other compounds that allow for generation of droplets even in channels of the width $w = 2$ mm.

It is worth noticing (Figure 1) that for practical purposes – as, e.g., performing syntheses inside droplets – the discrepancies between the volume (length) of the droplets formed at $Ca > 10^{-2}$ and the simple model $L \propto Ca^{-0.11}$ are not significant. The limits of throughput of formation of droplets are thus set not by the scaling of the volume of droplets with the speed of flow but rather by the transition from a dripping mode (of formation of droplets) to a jetting regime (in which the process of formation of droplets is no longer stable and amenable to precise control) [58–61].

2.2. Maximum Throughput of Formation of Droplets. In order to find the maximum rate of flow $Q_{max\ formation}$ for different widths of the channels, we performed a set of experiments that monitored the transition between the dripping and the jetting regimes. During each run of experiments, we measured the maximum length of the tip of the stream of the droplet phase L_t (Figure 2) and the length of droplet L_d as a function of speed of flow (Q_d/Q_c was fixed to 1.2).

In the dripping regime, $(L_t - L_d)/w = 1$. Upon transition to the jetting regime, $(L_t - L_d)/w$ increases abruptly. The plots in Figure 2 show the values Q_{jet} of Q_c at which $(L_t - L_d)/w$ crosses the value of 3 (which we assume arbitrarily as an onset of jetting). Both for the T-junction system and for the flow-focusing system (see SI, Figure S2), these values scale with the width

of the channel as $Q_{max\ formation} = Q_{jet} \propto w^{4/3}$, thus, providing much weaker scaling of the maximum rate of flow with the width of the channel than $Q \propto w^2$ as could be expected from considerations based on a capillary number controlled process and stronger than $Q \propto w$ as could be expected for a Reynolds number controlled mechanism.

2.3. Rate of Mixing in Droplets. A liquid plug translating through a capillary develops convection rolls inside. In curved channels, the convection rolls are asymmetric with respect to the centerline of the droplet. Switching of the curvature can be used to effectively mix the content of the droplet [62]. As shown by Song et al. [62], the flow inside the droplet resembles the "bakers transformation" and decreases the characteristic size of unmixed domains exponentially in the path travelled by the droplet. This leads to the following scaling for the time of mixing: $t_{mix} \propto (aw/u_d) \ln(Pe)$, where a is the dimensionless length of the droplet, u_d — the speed of the droplet, and Pe is the Peclet number (Pe $= wu_d/D$, where D is the diffusion constant of the molecule of interest). This scaling was previously verified experimentally for channels of widths ranging from 10 to 100 µm [62]. Here, we verified experimentally if the same scaling can be found in larger channels, i.e., if, at larger length scales, any other mechanisms might modify the scaling relationship for the time required to mix the content of a droplet.

We constructed chips ($w \in (0.2, 2)$ mm) that allow to monitor the mixing process in droplets via in-situ spectrophotometric measurements (Figure S3). This system combines two streams, one containing potassium thiocyanate (molar concentration 0.018 M; Chempur) and second containing iron(III) chloride (molar concentration 0.018 M, pH 5.5; Chempur) immediately

upstream of the orifice of the flow-focusing junction. As the two reagents mix, they form a complex (see reaction R1) that absorbs strongly at 470 nm and generates an intensively red color (Figure 3).

$$[Fe(H_2O)_6]^{3+}(aq) + SCN^-(aq) \rightarrow [Fe(H_2O)_5SCN]^{2+}(aq) + H_2O \quad (R1)$$
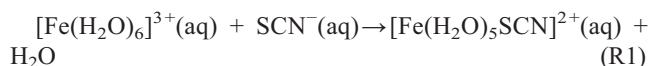
We used the USB 2000+ Ocean Optics fiber optic spectrophotometer connected to the microfluidic channel via multimode fibers BFH22-365 (0.22 NA, spectral range: 190–1200 nm, 365 μm core). We measured the absorption at a range of distances (after 5th, 10th, 15th 20th, 25th, 30th, 40th, 50th, and 60th meander) for a range of rates of flow of the liquids. As mixing and reaction proceeds, the absorbance at 470 nm increases to saturate (see SI, Figure S4) at a roughly constant value. We quantified the rate of mixing by measuring the time t_{90} after which the absorbance crossed over 90% of the saturation value. These results (Figure 4) confirm that the scaling proposed by Song et al. [62] holds for channels as large as 2 mm in width.

2.4. Maximum Throughput of Mixing. From the above results, it follows that the time required for mixing scales as $t_{mix} \propto (w^3/Q) \ln(Q/wD)$. Thus, the distance that the droplets need to travel for their content to be mixed scales as $L_{mix} = t_{mix} Q w^{-2} \propto w \ln(Q/wD)$. In a chip, the length that the droplet can travel is limited to the length of the channel (L_{ch}). By substituting L_{mix} with L_{ch}, we obtain the maximum rate of flow at which the content of the droplets is mixed within the chip: $Q_{max\ mixing} \propto wD\exp(L_{ch}/w) \propto wD\exp(N)$, where N is the number of meanders of the channel and is constant for a fixed geometry of the chip. We verified this result directly by monitoring the rate of flow at which the absorbance from the iron thiocyanate complex at the 40th meander started to fall below the maximum value (Figure S5 in SI). The result (Figure 4) confirms the postulated scaling of $Q_{max\ mixing} \propto w$.

2.5. Rate of Extraction. Liquid–liquid extraction is a technique used in chemical engineering [63], biology [64], environmental sciences [65, 66], and analytical chemistry [67, 68]. Miniaturization and reproducibility of the size of the droplets are both beneficial in this process because large surface-to-volume ratios speed up diffusion across the interface and because the processes can be well controlled [69]. According to Young et al. [70], there are two steps of extraction: (1) first, the concentration of the compound diffusing through the interface is homogenized along the streamlines that pass close to the
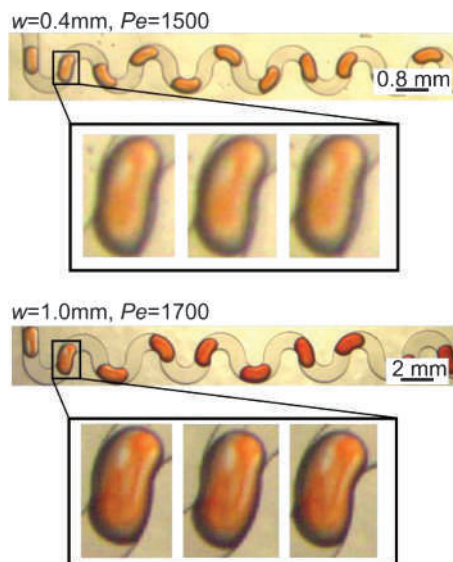
Figure 3. Visualization of mixing patterns for different widths of the channel at similar values of the Peclet number
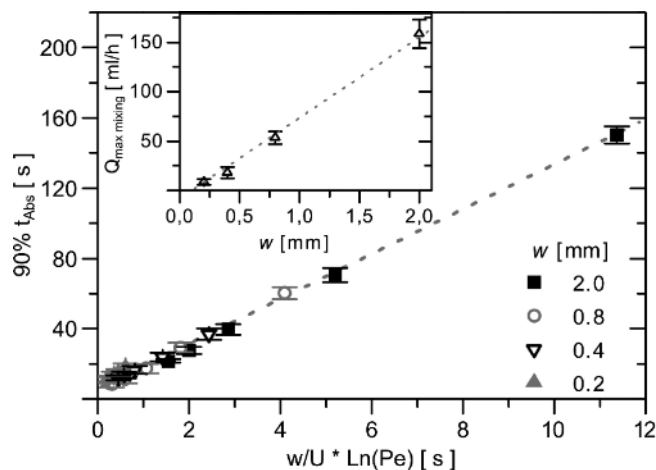
Figure 4. Scaling of the time of mixing in channels of different width. The inset shows the linear scaling of the maximum rate of flow for mixing with the width of the channel

interface, and later (2), the solute diffuses normally to the streamlines. Mary et al. [16] translated this mechanism into the following relation for the time of extraction: $t_{ext} \propto t_D Pe^{-2/3} (C_{inf}/C(t^*))$ where $t_D = w^2/D$ (w is typical length — in our case, the width of the channel), $C(t^*)$ is the averaged concentration in the closed zone around the droplet, and C_{inf} is the final concentration of solutes in the accepting liquid. Mary et al. [16] verified this scaling experimentally for channels of constant width (205 μm) and height varied between 30 and 95 μm, using the height of the channel as the characteristic length for diffusion. We used the same channels as for the quantification of mixing to monitor the rate of extraction. Droplets contained an aqueous buffer (phosphate buffer saline, PBS, pH=7.4, 10 M, Sigma-Aldrich) and extracted a solute (fluorescein sodium salt, $c=10^{-4}$ mol/cm^3; Sigma-Aldrich) dissolved in the continuous phase (1-octanol, Sigma-Aldrich, HPLC grade). We monitored the rate of extraction by monitoring the intensity of fluorescence with a charge-coupled device (CCD) camera mounted on a stereoscope equipped with a Mercury lamp. We analyzed the images to find L_e — the characteristic distance at which the brightness of droplets equaled the brightness of the continuous liquid, marking a well-defined point in the extraction process.

The time, t_e, which is needed for the droplet to travel the distance L_e is $t_e \propto L_e w^2/Q$. Please note that t_e is not the time needed to complete extraction. Indeed, droplets can be brighter
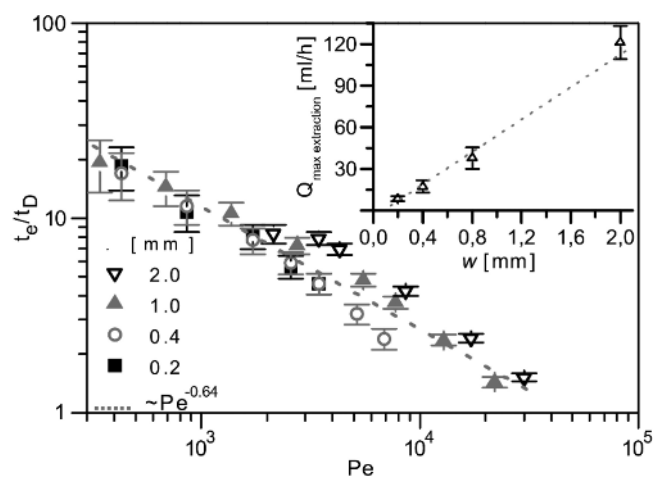
Figure 5. Scaling of the time of extraction, t_e, in channels of different width. Inset shows the linear scaling of the maximum rate of flow for extraction to proceed to the characteristic point of equalization of absorbance within the droplet and the continuous liquid

than the continuous liquid. t_e is only a convenient characteristic time of the extraction process and should be proportional to t_{ext}. Figure 5 shows t_e normalized by $t_D = w^2/D$ as a function of the Peclet number, Pe. Our results confirm the scaling postulated by Mary [16] yet for widths of the channels as large as 2 mm.

2.6. Maximum Throughput of Extraction. As the time of extraction scales as $t_{ext} \propto D^{-1/3} Q^{-2/3} w^{8/3}$, the length, L_{ext}, of the channel within which the extraction concludes is proportional to $L_{ext} \propto t_{ext} Q w^{-2} = D^{-1/3} Q^{1/3} w^{2/3}$. Substituting $L_{ch} = Nw$ (where N is a number of meanders of the channel) for L_{ext}, we obtain the maximum rate of flow for extraction $Q_{max\ extraction} = N^3 Dw$. Please notice that, for geometrically similar devices, the number of meanders N does not depend on the size of the channels. Thus, the maximum rate of flow for extraction is proportional to the width of the channel: $Q_{max\ extraction} \propto w$.

In order to test this relation, we recorded at a fast rate (1 kHz) the absorbance at 490 nm and at 500 nm at the 40th meander of the microfluidic systems. Thanks to the solvatochromic transition, the fluorescein salt dissolved in water presents the maximum absorbance at 490 nm while, when dissolved in oil, it absorbs strongest at 500 nm. At low rates of flow, extraction completes before the 40th meander and the oil absorbs more than the droplets. At fast rates of flow, extraction does not complete and the droplets absorb more than oil. In our experiments, we recorded the rate of flow for which the difference between the absorption at the two characteristic wavelengths vanished (see inset in Figure 5 and Figure S6 for details) and this rate of flow exhibits a linear relation to the width of the channel, as shown in the inset of Figure 5.

2.7. Chemical Reactions in Droplets. Mixing brings the substrates together at the molecular level, a prerequisite to initiate a chemical reaction. The yield of reaction depends on both: (1) the rate of mixing of substrates and (2) the rate of the chemical reaction. The kinetics is specific for a given reaction; therefore, the optimization of the process can be made only by adjusting the efficiency of mixing. Both mentioned rates can be associated with the characteristic times such as: t_{mix} — for mixing and τ_r — for reaction. As it was demonstrated above, the characteristic time for mixing inside a droplet is given by: $t_{mix} = 4.8\ (w^3/Q)\ \ln(Q/wD)$. This estimates the time that is required for homogenization of reactants within a droplet.

Characteristic reaction time, τ_r, provides an estimate of the time, within which the reaction is completed (starting from the ideal homogenization of substrates). This time can be approximated by half-life of the reaction. The Damköhler number (Da) is the dimensionless number that relates the rate of mixing to the rate of reaction. There are several forms of Damköhler number and most suitable for the description of the reaction conducted in microfluidic droplets reads: $Da = t_{mix}/\tau_r$.

There are three interesting regimes delineated by the value of Da: (1) mixing is much faster than the reaction ($Da \ll 1$), (2) the rate of mixing and the rate of reaction are comparable ($Da = 1$), and (3) reaction is faster than mixing ($Da \gg 1$). In the case of fast reactions ($Da \gg 1$), we can expect that the progress of the reaction is determined solely by the extent of mixing. Indeed, the substrates react as soon as they are mixed. In this regime, the process completes once the content of the

droplet is homogenized. Hence, this regime is perfect for quantification of the time of mixing. This fact was taken into account in analysis of mixing (see Section 2.3) by the choice of the reaction (see reaction R1). The half-life of this reaction is about 0.003 s [71], while the mixing time in all experimental runs was much longer: $t_{mix} \gg 1$ s, that results in large value of Da.

For $Da = 1$, the situation is much more complicated. The processes of mixing and chemical reaction are concurrent. While a fraction of the substrates are already mixed, they react and are mixed with the rest of the volume of the droplet. This creates complex kinetics in which the state of the droplet depends on the history of both mixing and reaction. The detailed quantitative description of this process is difficult. However, we can estimate the time needed to complete the reaction. We can expect that the prerequisite for the completion of reaction is homogenization of the compounds inside the droplet. This requires time not shorter than the time t_{mix} that was considered above. Once reagents are distributed uniformly inside a droplet, the progress of reaction depends only on its own chemical kinetics. We can estimate the extent of time required to complete the reaction to be no longer than reaction timescale, τ_r. Summarizing, we can assume that the reaction should be completed within the time between t_{mix} and $t_{mix} + \tau_r$.

From the practical point of view, the most interesting case is the regime defined by $Da \ll 1$. Because of relatively fast mixing and slow reaction, we can assume that the reaction starts after complete mixing. Hence, at the beginning of reaction, the compounds are homogenized within the whole volume of a droplet and reaction proceeds uniformly inside a droplet. Moreover, the time of homogenization is short when compared to the time of reaction, so it can be neglected. This implies that the stage of reaction depends solely on the time measured starting from generation of a droplet. As the residual time corresponds to the position of a droplet in the microfluidic channel, the stage of reaction depends on the length of the device and the rate of flow.

We tested the predictions for the throughput of an actual synthesis in terms of the yield of the reaction as a function of the rate of flow-through geometrically similar systems of various widths of the channels. We conducted the synthesis of pyrrole by reacting 2,5-hexanedione (Sigma) with ethanolamine (Sigma) in microdroplets on the chip (see Figure 6) [72]. We generated droplets from a compound stream formed by two incoming solutions of the substrates delivered directly into a FF-junction (SI, Figure S3). As an immiscible carrier liquid, we used Fluorinert FC-40 (3 M). We run the same process in four chips with different widths of the square cross-section channels $w = 0.4$, 1.0, 1.5, 2.0 mm. We quenched the reaction at the moment of droplets exiting the reaction channel (after the 50th meander) by coalescing the droplets with acetone. The input solution of 2,5-hexanedione contained an internal standard (3,5-dimethylphenol, Sigma). This allowed us to quantify the yield of the reaction by running the collected samples through an HPLC analyzer (Beckman with RID-6A Shimadzu refractive index detector).

We can estimate the timescale of synthesis of pyrrole on the basis of known reaction rate constant for synthesis at
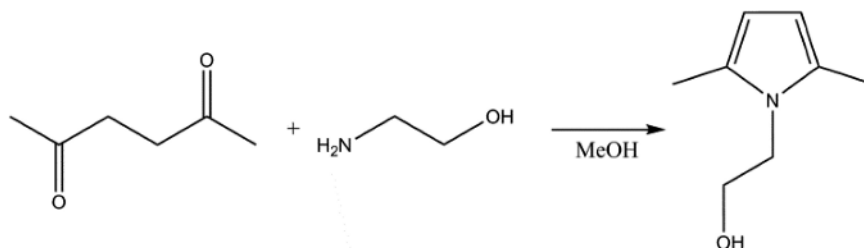
Figure 6. Paal–Knorr pyrrole synthesis

75 °C ($k=5.4\cdot10^{-3}$ L/mol/s) [73]. The half-life for synthesis is about 130 s, and we can expect that it is even longer in the case of the same reaction conducted at room temperature. On the other hand, we know that the mixing time can be estimated from the equation $t_{mix}=4.8$ (w^3/Q) $\ln(Q/wD)$. This allowed us to estimate time of mixing in experiments on synthesis of pyrrole, which was no longer than 5 s. Hence, the Damköhler number was not greater than 0.04 — a value small enough to assume that the mixing time can be neglected.

The dimensionless length of the devices was kept constant (i.e., the actual length scaled with the width of the channel), and the residual time was controlled by the change of the rate of flow. The time was estimated on the basis of the length of the device ($L_{ch}=Nl_mw$, where $N=$const$=50$ is a number of meanders and $l_m=4.71$ is a dimensionless length of a single meander) and the rate of flow (Q): $t=L_{ch}w^2/Q=Nl_mw^3/Q$. The order of the tested reaction is above one; therefore, the reaction yield has the form of an exponential curve in time. The dependence of the yield of reaction is shown in Figure 7. One can see that the measured yield follows the exponential curve according to our expectation for small Damköhler number.

Efficient mixing inside a droplet in microfluidic chip allows conducting reactions for small Damköhler number, providing for superior control over the kinetics of reactions. This feature may be very relevant for consecutive reactions as it enables to quench the reaction at any precisely chosen time and allow to obtain select products of reaction.

2.8. Maximum Throughput of Reaction. The limit of low Da simplifies the design of the device, when we want to maximize the throughput while maintaining the requested yield of the synthesis. Damköhler number decreases with an increasing rate of flow, Q: Da$=t_{mix}/\tau_r \propto (w^3/Q)$ $\ln(Q/wD)/\tau_r$. As a result, maximization of the rate of flow (Q) does not change the low Da regime. Indeed, increasing the rate of flow decreases the time of mixing, while the reaction time, τ_r, is constant for a given reaction.

For a given required time of residence of the reagents in the system, i.e., the time, t_{req}, that is required for the reaction to proceed to the requested yield, we can calculate the rate of flow of the liquids as a function of the geometrical dimensions of the channels. The time of residence is simply proportional to $t_{req} \propto (L_{ch}w^2)/Q$, and for geometrically similar systems, the length of the channel is proportional to its width ($L_{ch} \propto w$), yielding $t_{req} \propto w^3/Q$. Thus, for a given fixed value of t_{req}, the rate of flow scales with the cube of the width of the channel $Q \propto w^3$.

As a consequence, the reaction itself does not impose the limit on the throughput of the system because the limitations on the rate of formation ($Q_{max\ formation} \propto w^{4/3}$) and mixing ($Q_{max\ mixing} \propto w$) are more stringent. In the case of Da$\ll 1$, mixing is faster than reaction and the throughput of synthesis will be limited by the rate of formation of droplets ($Q_{max\ reaction} \propto w^{4/3}$), while for Da$=1$ and Da $\gg 1$, mixing ($Q_{max\ reaction} \propto w$) will set the limit.

Hence, in practice, the Damköhler number for maximum rate of flow obeys the following scaling law: Da $\propto w^{5/3}$ $\ln(Q/wD)/\tau_r$. The fact that Da increases with the width of the channel roughly like $w^{5/3}$ should be taken into account as the scaling up of the devices may change the regime for conducting reaction and the above consideration for low Da limit may not apply. However, changing the width of the channel 10 times would increase the Damköhler number roughly 46 times. Hence, for very slow reaction, e.g., when Da is about 10^{-3}, we can scale up the device up to 10 times keeping Da very low.

2.9. Optimization for Throughput

2.9.1. Geometrical Similarity. The observation that the maximum rates of flow for (1) mixing and (2) extraction both scale linearly with the width of the channel, and that increasing the rate of flow in proportion to the width of the channel guarantees stability of formation of droplets, has an important consequence for the design of microfluidic systems for optimized throughput. Given the specific choice of the reactants and carrier liquids (e. g., diffusion constants), it is enough to optimize the geometry and length of the channel that allows for mixing and/or extraction at the maximum rate (say Q_1) of formation of droplets at one scale of the channels (say w_1). Once such a geometry is known, it can be simply scaled to different dimensions. Both the geometrical dimensions of the channels (i.e., the layout of the network of fluidic ducts) and the rates of flow can be simply multiplied by the same number (i.e., $w_2=\alpha w_1$ and $Q_2=\alpha Q_1$), and the system will operate as effectively (i.e., optimally in terms of throughput) as the original one.

Since the maximum rate of flow for formation of droplets scales slightly faster with w than w^1 (i.e., $Q_{max\ formation} \propto w^{4/3}$), larger systems can be made accordingly slightly longer (in terms of the length of the channel divided by its width) to fully take advantage of the maximum throughput. If Q_2 is chosen as $Q_2=Q_1$ $(w_2/w_1)^{4/3}$, then for mixing, the number N_2 of meanders in the second device should be: $N_2=N_1$ $\ln(Cw_2)/\ln(Cw_1)$, where C is a constant (/m), and for extraction, $N_2=N_1$ $(w_2/w_1)^{1/9}$.
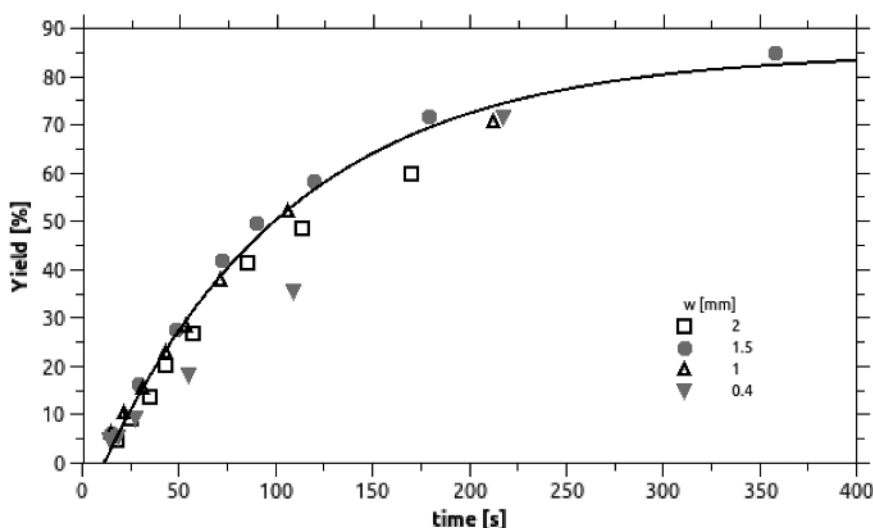
Figure 7. Dependence of the reaction yield on the time for different width of channels. The solid line shows the exponential fit: Yield$=(0.89–0.95\exp(−\text{time}/99$ s$))\cdot100\%$

The scaling of the maximum rate of flow for chemical synthesis in the limit of low Da is: $Q_{\text{max reaction}} \propto w^3$; however, practically, it is limited by the scaling of formation of droplets: $Q_{\text{max formation}} \propto w^{4/3}$. Indeed, the system cannot operate properly in condition when reproducible generation of droplets is not ensured. However, for geometrically similar systems, the increase of the width of a channel would be still more beneficial for the throughput than in the case of extraction or mixing.

2.9.2. Throughput versus the Cost of Fabrication. Whatever is the length of the channel that is required for mixing or extraction, for geometrically similar systems, it is proportional to the width of the channel. Thus, the surface area A_{ch} occupied by a single channel is proportional to w^2. Then, the throughput T per unit area is proportional to $Q_{\text{max}}/A_{\text{ch}} \propto w^{-1}$ in the case of mixing and extraction. The scaling of T is slightly weaker for reaction in the limit of low Da: $T = Q_{\text{max formation}}/A_{\text{ch}} \propto w^{-2/3}$.

The observation that the maximum throughput per unit area of the chip decreases in inverse proportion to the width of the channel can serve as a useful guideline in designing the chips and technology for optimized throughput. Maximization of throughput can be best realized via parallelization of small channels. Decreasing the size of the channels, however, increases the cost and difficulty of fabrication of the chips and maintenance of the process. Smaller channels impose more stringent requirements on filtering. Also, the pressure head needed to drive the liquids at the maximum rate of flow ($Q_{\text{max}} \propto w$) increases for smaller channels $\Delta p \propto w^{-2}$ (because the length of the channel $L \propto w$, hydraulic resistance $R \propto Lw^{-4}$ and $\Delta p \propto Q_{\text{max}}R$). Thus, for a given set of technologies available to a laboratory or industrial entity, their effective cost can be calculated to provide for the optimum choice of the scale of the channels for given application.

2.9.3. Throughput of a Single Junction. Optimization of the throughput via parallelization of small channels may be beneficial in mass production applications. Even if the cost of fabrication is high, the relative cost may be attractive when compared to the yield over the life time of the flow reactor. On the other hand, there may also be applications in which an amount of a specific product must be synthesized with high quality. The throughput itself may not be the primary concern, while the amount of product is too high to be produced with a micrometric droplet system. In these applications, it may be advantageous to use a single device with large channels. Millimetric channels (e.g., $w=1$ mm) can yield substantial throughputs (e.g., 100 mL/h) that can be sufficient for small-scale laboratory syntheses that can profit from all the advantages of conducting reactions in the microfluidic droplet format and use inexpensive fabrication of millimetric channels.

2.9.4. Limitations Set by Kinetic Requirements. It may be the case that a reaction of interest requires the time of mixing to be shorter than a given threshold, t_{req} (i.e., in formation of nanoparticles of specific mean diameter and variance) [53]. Such limitation combined with the scaling of the maximum rate of flow in channels of given width translates into a limitation on the maximum width of the channel for geometrically similar systems (the number of meanders N is fixed). The time of mixing is given by $t_{\text{mix}} \propto (w^3/Q) \ln(Q/wD)$ (for our system, the constant of proportionality in this equation is equal to 4.8, similar in value ($\approx$3) to the one that we estimated for the results by Song et al. [9]). Substituting $Q = Q_{\text{max mixing}} \propto wD\exp(N)$ and t_{req} for t_{mix}, we obtain: $w_{\text{max mixing}}^2 \propto t_{\text{req}}D\exp(N)/N$, where $w_{\text{max mixing}}$ is the maximum width of the channel in which the reaction can be conducted. This result also provides the maximum rate of flow as a function of the maximum time of mixing as $Q_{\text{max mixing}}(t_{\text{req}}) \propto t_{\text{req}}^{1/2}D^{3/2}\exp(N)^{3/2}N^{-1/2}$. Setting a limitation on the time of extraction sets a similar limit on $w_{\text{max extraction}}(t_{\text{req}})^2 \propto D^{1/3}t_{\text{req}}$ and $Q_{\text{max extraction}}(t_{\text{req}}) \propto D^{-1/6}t_{\text{req}}^{1/2}$.

For example, it is universally accepted that the growth of semiconducting nanocrystals is characterized by the diffusion-limited Ostwald ripening process, as reported for TiO2 [74], InAs, and CdSe [75]. Hartlieb et al. [76] have shown that the speed of mixing determines the diameter of the synthesized ZnO nanoparticles. For example, obtaining particles of diameter of 1.5 nm required mixing to be completed within 170 ms. Substituting this value into the equation for t_{mix} yields the maximum width of the channel that can be used for such synthesis $w_{\text{max}}=460$ μm and the corresponding $Q_{\text{max}}=17.2$ mL/h.

3. Conclusions

We have verified experimentally the scaling laws for formation of droplets, mixing in droplets, extraction from droplets, and reaction within droplets in microfluidic and milifluidic channels characterized by widths ranging from 200 μm to 2 mm. Our analysis includes the first direct experimental verification of the scaling of the size of droplets and the dripping–jetting transition with the size of the channels and the rates of flow of the liquids. We have also, for the first time, verified experimentally the scaling relation proposed by Song et al. [62] for mixing across the millimetric scale of the channels. Our results confirmed this scaling for the flow of droplets in channels up to 2 mm in width. Similarly, for extraction, our experiments extended the use of the relation developed by Mary [16] for channels up to 2 mm in width. Finally, we have analyzed the rate of synthesis against the value of the Damköhler number and tested the resulting relations experimentally.

On the basis of the experimentally verified scaling relations for the individual processes, we have provided comprehensive overview of the scaling of the chemical syntheses in droplet flow reactors. Our results show that the maximum throughput can be obtained with the smallest channels and in parallel systems. We have also derived for the first time the scaling of mass-throughput of chemical syntheses per unit area of the chip. We also show how this relation can be used to optimize throughput of the droplet flow reactors against the cost of production and maintenance of microfluidic chips comprising channels of different dimensions.

The observation that the size of the channels (and volumes of the droplets) can be scaled up, while sustaining the level of control and efficiency that was observed for small channels, is important because (1) some processes are more effective in larger volumes (as, e.g., crystallization of proteins [77, 78]) and (2) large (i.e., millimetric) channels can provide a convenient vista to controlled laboratory syntheses conducted inside droplets.

The paper focuses on the fundamental physical mechanisms that underlay chemical reactions conducted in droplets. In addition to the proper design of the geometry of the droplet reactors, execution of chemical syntheses in droplets requires meeting a number of technical requirements. These will depend on the type of solvents, reactants, and conditions for the particular reaction. One of the critical conditions for proper operation of droplet reactors is that the droplets do not wet (i.e., contact) the walls of the channels. The droplets should always be separated from these walls by thin wetting films of the continuous liquid. This condition was satisfied in our experiments in which we used devices fabricated in either polycarbonate or polydimethylsiloxane. The wetting properties are crucial for stable formation of droplets and their transport through the channels. Hydrophobic channels are required for aqueous droplets carried in an oily continuous liquid. Conversely, hydrophilic channels are needed for oily droplets immersed in an aqueous continuous phase. The requested wetting properties may be achieved by the

use of surfactants and via appropriate modification of the surface chemistry of the channels. In this way, the most popular and nonexpensive microfabrication techniques, such as soft lithography (PDMS) and micro milling (e.g., polycarbonate), may be used together with an appropriately selected coating method. The appropriate choice of materials should potentially also consider resistance to high temperatures and aggressive solvents. The materials, coating methods, and surfactants are discussed in detail in a review by Seemann et al. [79].

4. Experimental

4.1. Microfabrication. We fabricated the chips via direct milling in polycarbonate (PC) sheets (Macroclear, Bayer, Germany) of various thicknesses using a CNC milling machine (Ergwind, Poland). The CNC machine has a reproducibility of positioning of 5 μm and allows for using milling bits as small as 100 μm in diameter. We bounded the milled microchip with a flat slab of polycarbonate using method elaborated by Ogończyk et al. [80].

For the ultraviolet (UV) measurements needed to quantify mixing and extraction, we fabricated the devices in polydimethylsiloxane (PDMS) using the milled microchips to create a master in PDMS. After that, the PDMS master was coated with silane [81] and used to mould PDMS replicas of the original PC plates. These were then bonded [81] with flat pieces of PDMS.

4.2. Absorption Measurements. We used the Ocean Optics USB 2000+ miniature fiber optic spectrometer interfaced with the chips via multimode fibers BFH22-365 (0.22 NA, spectral range: 190–1200 nm, 365 μm core) to measure the absorption of transparent phases (oil and water). We inserted fibers into the chip and connected them to a light source (DH2000-FHS-DUV) and detector. The lamp has both the deuterium and halogen bulbs yielding emission intensity between 210 and 1700 nm. We carried out the absorption data analysis in accordance to Lambert–Beer law in order to check mixing and extraction.

4.3. Measurements of Sizes of Droplets. We used a stereoscope Nikon SMZ1000 equipped with a CCD U-eye 2250SE-C camera (IDS, USA). We analyzed the sequences of images of droplets with a custom written script in MATLAB (MathWorks), which automatically recognized droplets and measured their sizes.

4.4. Flow Control. We used two techniques to feed the chips with liquids. In the experiments on formation of droplets, we used the precise system comprising of pressurized reservoirs of liquids interfaced with the chip via capillaries of high hydraulic resistance. The same system was examined and described in detail by Korczyk et al. [82] For the other experiments, we used syringe pumps PHD2000 (Harvard Apparatus, USA) with 1 mL syringes (BD) to reduce oscillations generated by syringe pumps [82]. For fluidic connections, we used the PE-60 tubing (Becton-Dickinson, USA).

4.5. Measurements of the Reaction Yield. The amounts of the compounds used for synthesis of pyrrole were as follows: (1) 2,5-hexanedione — Mw=114.14 g/mol, 1.600 g in 10.000 g (EtOH), molar concentration: 1.1 mol/L; (2) ethanolamine — Mw=61.08 g/mol, 0.820 g in 10.000 g (EtOH), molar concentration: 1.1 mol/L; (3) 3.5-dimethylphenol — Mw=122.16 g/mol, 0.800 g added to the solution of 2,5-heksanedion as an internal standard.

The reaction in droplets was quenched by coalescing the droplets with a stream of acetone washing the outlet of the microfluidic device. The output mixture was collected into the beaker, where two immiscible phases were separated via density difference. After that, 20 μL of the sample was used for quantification of the yield of the reaction with the use of the Beckman HPLC analyzer with RID-6A Shimadzu refractive index detector. We used the column ACE C18 (5 μm) with dimensions 250×4.6 mm. Mobile phase MeOH–water of 55:45 and flow rate of 1.0 mL/min were applied.

Supporting Information

Electronic Supplementary Material (ESM) is available in the online version at doi:10.1556/JFC-D-14-00038.

References

1. Skeggs, L. *Am. J. Clin. Pathol.* **1957**, *28*, 311–322.
2. Ruzicka, J.; Hansen, E. H. *Anal. Chim. Acta* **1975**, *78*, 145–157.
3. Ruzicka, J.; Hansen, E. H. *Anal. Chim. Acta* **1984**, *161*, 1–25.
4. Whitesides, G. M. *Nature* **2006**, *442*, 368–373.
5. Harrison, D. J.; Glavina, P. G.; Manz, A. *Sens. Actuators B Chem.* **1993**, *10*, 107–116.
6. Erickson, D.; Li, D. *Anal. Chim. Acta* **2004**, *507*, 11–26.
7. Thorsen, T.; Roberts, R. W.; Arnold, F. H.; Quake, S. R. *Phys. Rev. Lett.* **2001**, *86*, 4163–4166.
8. Anna, S. L.; Bontoux, N.; Stone, H. A. *Appl. Phys. Lett.* **2003**, *82*, 364–366.
9. Song, H.; Ismagilov, R. F. *J. Am. Chem. Soc.* **2003**, *125*, 14613–14619.
10. Teh, S.-Y.; Lin, R.; Hung, L.-H.; Lee, A. P. *Lab Chip* **2008**, *8*, 198–220.
11. Günther, P. M.; Möller, F.; Henkel, T.; Köhler, J. M.; Groß, G. A. *Chem. Eng. Technol.* **2005**, *28*, 520–527.
12. Song, H.; Chen, D. L.; Ismagilov, R. F. *Angew. Chem., Int. Ed.* **2006**, *45*, 7336–7356.
13. Theberge, A. B.; Courtois, F.; Schaerli, Y.; Fischlechner, M.; Abell, C.; Hollfelder, F.; Huck, W. T. S. *Angew. Chem., Int. Ed.* **2010**, *49*, 5846–5868.
14. Stankiewicz, A.; Moulijn, J. A. *Ind. Eng. Chem. Res.* **2002**, *41*, 1920–1924.
15. Lomel, S.; Falk, L.; Commenge, J. M.; Houzelot, J. L.; Ramdani, K. *Chem. Eng. Res. Des.* **2006**, *84*, 363–369.
16. Mary, P.; Studer, V.; Tabeling, P. *Anal. Chem.* **2008**, *80*, 2680–2687.
17. Yeo, L. Y.; Chang, H.-C.; Chan, P. P. Y.; Friend, J. R. *Small* **2011**, *7*, 12–48.
18. Washburn, A. L.; Bailey, R. C. *Analyst* **2010**, *136*, 227–236.
19. Harel, E. *Prog. Nucl. Magn. Reson. Spectrosc.* **2010**, *57*, 293–305.
20. Lewinski, J.; Bury, W.; Justyniak, I.; Lipkowski, J. *Angew. Chem., Int. Ed.* **2006**, *45*, 2872–2875.
21. Geyer, K.; Gustafsson, T.; Seeberger, P. *Synlett* **2009**, *2009*, 2382–2391.
22. Chang, C.-H.; Paul, B. K.; Remcho, V. T.; Atre, S.; Hutchison, J. E. *J. Nanoparticle Res.* **2008**, *10*, 965–980.
23. Brivio, M.; Verboom, W.; Reinhoudt, D. N. *Lab. Chip* **2006**, *6*, 329–344.
24. Wiles, C.; Watts, P.; Haswell, S. J.; Pombo-Villar, E. *Lab. Chip* **2001**, *1*, 100–101.
25. Skelton, V.; Greenway, G. M.; Haswell, S. J.; Styring, P.; Morgan, D. O.; Warrington, B. H.; Wong, S. Y. F. *Analyst* **2001**, *126*, 11–13.
26. Antes, J.; Boskovic, D.; Krause, H.; Loebbecke, S.; Lutz, N.; Tuercke, T.; Schweikert, W. *Chem. Eng. Res. Des.* **2003**, *81*, 760–765.
27. Doku, G. N.; Haswell, S. J.; McCreedy, T.; Greenway, G. M. *Analyst* **2001**, *126*, 14–20.
28. Panke, G.; Schwalbe, T.; Stirner, W.; Taghavi-Moghadam, S.; Wille, G. *Synthesis* **2003**, 2827–2830.
29. Loebbecke, S.; Tuercke, T.; Mendl, A.; Boskovic, D. 27th Army Science Conference, 2010.
30. Danckwerts, P. V. *Chem. Eng. Sci.* **1958**, *8*, 93–102.
31. David, R.; Lintz, H.-G.; Villermaux, J. *Chem. Ing. Tech.* **1984**, *56*, 104–110.
32. Nouri, L.; Legrand, J.; Benmalek, N.; Imerzoukene, F.; Yeddou, A.-R.; Halet, F. *Chem. Eng. J.* **2008**, *142*, 78–86.
33. Kurtanjek, Z. *Curr. Stud. Biotechnol. VOL II Environ.* **2001**, 89–95.
34. Slund, B. L. Å.; Rasmuson, Å. K. C. *AIChE J.* **1992**, *38*, 328–342.
35. Verschuren, I. L. M.; Wijers, J. G.; Keurentjes, J. T. F. *AIChE J.* **2001**, *47*, 1731–1739.
36. Fang, J. Z.; Lee, D. J. *J. Chem. Eng. Jpn.* **2000**, *33*, 923–926.
37. Nisisako, T.; Torii, T. *Lab. Chip* **2008**, *8*, 287–293.
38. Li, W.; Greener, J.; Voicu, D.; Kumacheva, E. *Lab. Chip* **2009**, *9*, 2715–2721.

39. Engl, W.; Backov, R.; Panizza, P. *Curr. Opin. Colloid Interface Sci.* **2008**, *13*, 206–216.

40. Engl, W.; Tachibana, M.; Panizza, P.; Backov, R. *Int. J. Multiph. Flow* **2007**, *33*, 897–903.

41. Panizza, P.; Engl, W.; Hany, C.; Backov, R. *Colloids Surf. Physicochem. Eng. Asp.* **2008**, *312*, 24–31.

42. Xu, S. Q.; Nie, Z. H.; Seo, M.; Lewis, P.; Kumacheva, E.; Stone, H. A.; Garstecki, P.; Weibel, D. B.; Gitlin, I.; Whitesides, G. M. *Angew. Chem., Int. Ed.* **2005**, *44*, 724–728.

43. Engl, W.; Tachibana, M.; Colin, A.; Panizza, P. *Chem. Eng. Sci.* **2008**, *63*, 1692–1695.

44. Steinbacher, J. L.; Lui, Y.; Mason, B. P.; Olbricht, W. L.; McQuade, D. T. *J. Flow Chem.* **2012**, *2*, 56–62.

45. Garstecki, P.; Gitlin, I.; DiLuzio, W.; Whitesides, G. M.; Kumacheva, E.; Stone, H. A. *Appl. Phys. Lett.* **2004**, *85*, 2649.

46. Garstecki, P.; Stone, H. A.; Whitesides, G. M. *Phys. Rev. Lett.* **2005**, *94*, 164501.

47. Garstecki, P.; Fuerstman, M. J.; Stone, H. A.; Whitesides, G. M. *Lab. Chip* **2006**, *6*, 437–446.

48. De Menech, M.; Garstecki, P.; Jousse, F.; Stone, H. A. *J. Fluid Mech.* **2008**, *595*, 141–161.

49. Christopher, G. F.; Noharuddin, N. N.; Taylor, J. A.; Anna, S. L. *Phys. Rev. E* **2008**, *78*, 036317.

50. Lee, W.; Walker, L. M.; Anna, S. L. *Phys. Fluids* **2009**, *21*, 032103.

51. Nie, Z.; Seo, M.; Xu, S.; Lewis, P.; Mok, M.; Kumacheva, E.; Whitesides, G.; Garstecki, P.; Stone, H. *Microfluid. Nanofluidics* **2008**, *5*, 585–594.

52. Van der Graaf, S.; Nisisako, T.; Schroën, C. G. P. H.; van der Sman, R. G. M.; Boom, R. M. *Langmuir* **2006**, *22*, 4144–4152.

53. Van Steijn, V.; Kleijn, C. R.; Kreutzer, M. T. *Lab. Chip* **2010**, *10*, 2513–2518.

54. Glawdel, T.; Elbuken, C.; Ren, C. L. *Phys. Rev. E* **2012**, *85*, 016322.

55. Glawdel, T.; Elbuken, C.; Ren, C. L. *Phys. Rev. E* **2012**, *85*, 016323.

56. Wehking, J. D.; Gabany, M.; Chew, L.; Kumar, R. *Microfluid. Nanofluidics* **2014**, *16*, 441–453.

57. Van Steijn, V.; Kreutzer, M. T.; Kleijn, C. R. *Chem. Eng. Sci.* **2007**, *62*, 7505–7514.

58. Guillot, P.; Colin, A. *Phys. Rev. E* **2005**, *72*, 066301.

59. Utada, A. S.; Fernandez-Nieves, A.; Stone, H. A.; Weitz, D. A. *Phys. Rev. Lett.* **2007**, *99*, 094502.

60. Guillot, P.; Colin, A.; Utada, A. S.; Ajdari, A. *Phys. Rev. Lett.* **2007**, *99*, 104502.

61. Fu, T.; Wu, Y.; Ma, Y.; Li, H. Z. *Chem. Eng. Sci.* **2012**, *84*, 207–217.

62. Song, H.; Bringer, M. R.; Tice, J. D.; Gerdts, C. J.; Ismagilov, R. F. *Appl. Phys. Lett.* **2003**, *83*, 4664–4666.

63. Seiler, M. *Fluid Phase Equilib.* **2006**, *241*, 155–174.

64. Kroner, K. H.; Hustedt, H.; Kula, M.-R. *Biotechnol. Bioeng.* **1982**, *24*, 1015–1045.

65. Baxter, D. C.; Frech, W. *Pure Appl. Chem.* **1995**, *67*, 615–648.

66. Hasegawa, M.; Sabatini, D.; Harwell, J. *J. Environ. Eng.* **1997**, *123*, 691–697.

67. Hendriks, G.; Uges, D. R. A.; Franke, J. P. *J. Chromatogr. B* **2007**, *853*, 234–241.

68. Maruyama, T.; Nakashima, K.; Kubota, F.; Goto, M. *Anal. Sci.* **2007**, *23*, 763–765.

69. Squires, T. M.; Quake, S. R. *Rev. Mod. Phys.* **2005**, *77*, 977–1026.

70. Young, W.; Pumir, A.; Pomeau, Y. *Phys. Fluids Fluid Dyn.* **1989**, *1*, 462–469.

71. Chance, B. *J. Frankl. Inst.* **1940**, *229*, 737–766.

72. Nieuwland, P. J.; Segers, R.; Koch, K.; van Hest, J. C. M.; Rutjes, F. P. J. T. *Org. Process Res. Dev.* **2011**, *15*, 783–787.

73. Wiles, C.; Ngamsom, B.; Stemmet, C. *The Use of Micro Reactors for the Extraction of Kinetic Information from Synthetic Reactions and Application to the Paal–Knorr Pyrrole Synthesis*; Chemtrix, 2011.

74. Oskam, G.; Nellore, A.; Penn, R. L.; Searson, P. C. *J. Phys. Chem. B* **2003**, *107*, 1734–1738.

75. Peng, X. G.; Wickham, J.; Alivisatos, A. P. *J. Am. Chem. Soc.* **1998**, *120*, 5343–5344.

76. Hartlieb, K. J.; Raston, C. L.; Saunders, M. *Chem. Mater.* **2007**, *19*, 5453–5459.

77. Manuel García-Ruiz, J. *J. Struct. Biol.* **2003**, *142*, 22–31.

78. Bodenstaff, E. R.; Hoedemaeker, F. J.; Kuil, M. E.; de Vrind, H. P. M.; Abrahams, J. P. *Acta Crystallogr. D Biol. Crystallogr.* **2002**, *58*, 1901–1906.

79. Seemann, R.; Brinkmann, M.; Pfohl, T.; Herminghaus, S. *Rep. Prog. Phys.* **2012**, *75*, 016601.

80. Ogończyk, D.; Węgrzyn, J.; Jankowski, P.; Dąbrowski, B.; Garstecki, P. *Lab. Chip* **2010**, *10*, 1324–1327.

81. Duffy, D. C.; McDonald, J. C.; Schueller, O. J. A.; Whitesides, G. M. *Anal. Chem.* **1998**, *70*, 4974–4984.

82. Korczyk, P. M.; Cybulski, O.; Makulska, S.; Garstecki, P. *Lab. Chip* **2011**, *11*, 173–175.